JCTC Journal of Chemical Theory and Computation

Molecular Dynamics Simulations of Proteins: Can the Explicit Water Model Be Varied?

David R. Nutt*,† and Jeremy C. Smith†,‡

Computational Molecular Biophysics, IWR, Im Neuenheimer Feld 368, University of Heidelberg, 69120 Heidelberg, Germany, and Center for Molecular Biophysics, Oak Ridge National Laboratory/University of Tennessee, P.O. Box 2008, 1 Bethel Valley Road, Oak Ridge, Tennessee 37831

Received March 6, 2007

Abstract: In molecular mechanics simulations of biological systems, the solvation water is typically represented by a default water model which is an integral part of the force field. Indeed, protein nonbonding parameters are chosen in order to obtain a balance between water−water and protein−water interactions and hence a reliable description of protein solvation. However, less attention has been paid to the question of whether the water model provides a reliable description of the water properties under the chosen simulation conditions, for which more accurate water models often exist. Here we consider the case of the CHARMM protein force field, which was parametrized for use with a modified TIP3P model. Using quantum mechanical and molecular mechanical calculations, we investigate whether the CHARMM force field can be used with other water models: TIP4P and TIP5P. Solvation properties of N-methylacetamide (NMA), other small solute molecules, and a small protein are examined. The results indicate differences in binding energies and minimum energy geometries, especially for TIP5P, but the overall description of solvation is found to be similar for all models tested. The results provide an indication that molecular mechanics simulations with the CHARMM force field can be performed with water models other than TIP3P, thus enabling an improved description of the solvent water properties.

Introduction

Water plays an essential role in all living organisms. Enzymes, for example, require a certain level of hydration before they can perform their biological function.[1] Therefore, it is important that biomolecular simulations should try and recreate the aqueous environment of biomolecules as accurately as possible by including the effects of water, either implicitly or explicitly.

Most modern molecular mechanics (MM) force fields, such as CHARMM,[2] AMBER,[3] and GROMOS,[4] are typically designed for use with a specific water model, chosen during the parametrization process. The OPLS-AA force field is slightly different, since it is designed to be compatible with three different water models.[5] The majority of biomolecular simulations are then performed using the default water model. However, for any given simulation, the question arises as to whether the water model is suitable under the precise simulation conditions. In the case of biological systems under physiological conditions, the default description of water is probably satisfactory. However, this is probably not the case for simulations at low temperatures or high pressure, for example.

Ideally, one should be able to select the most appropriate water model for the chosen simulation conditions in order to obtain the best possible description of the system being studied. However, in practice, as the water model is an integral part of the force field, it is possible that simply

* Corresponding author phone: +49-6221-548805; fax: +49-6221-548868; e-mail: david.nutt@iwr.uni-heidelberg.de.
† University of Heidelberg.
‡ Oak Ridge National Laboratory/University of Tennessee.

10.1021/ct700053u CCC: $37.00
Published on Web 05/25/2007

changing the water model will lead to an imbalance in the protein−water and water−water interactions. However, this issue has not yet been investigated.

In the main part of this paper, we investigate the effect of using different water models on the solvation properties of a number of small molecules and a small protein described with the CHARMM force field. Before this, it is instructive to consider water models themselves and the central role of the water model in the parametrization of biomolecular force fields.

Models for Water. In the development and parametrization of water models, two separate approaches can be identified. The first supposes that if the details of the interactions (electrostatic, repulsive, and dispersion interactions, for example) between two atoms or molecules can be correctly described (for example, by reproducing high-level ab initio calculations), the resulting potential will also be suitable for describing larger clusters as well as all possible phases. An example of such a potential is provided by the family of anisotropic site−site potentials (ASP) for water developed by Stone and co-workers.[6−8] Although these so-called ab initio interaction potentials have yielded insight into the structure and properties of small water clusters[9] and the adsorption of water on surfaces,[10−12] they suffer from being computationally intensive, leading to limitations in their fields of application (at least with current computational resources).

Alternatively, the potential can be parametrized in order to reproduce bulk properties for a chosen phase under given conditions. This empirical approach gave rise to the family of Transferable Intermolecular Potentials (TIP) developed by Jorgensen and co-workers: TIP3P,[13] TIP4P,[13] and TIP5P.[14] Other widely used empirical water models include the Simple Point Charge models developed by Berendsen and co-workers (SPC[15] and SPC/E[16]) and the Stillinger and Rahman model (ST2).[17] These models describe bulk liquid water with varying degrees of accuracy.[18] However, they are not capable of correctly describing small clusters or other phases since they were neither designed nor parametrized for these purposes. Biomolecular simulations typically employ empirical water models due to their computational efficiency.

Water as a Solvent in Biological Systems. Early biomolecular simulations were carried out either in vacuum or in an environment of fixed dielectric constant in order to reduce the computational expense. In most modern simulations, however, water is explicitly included in order to describe the system as completely as possible. In some cases, such as very large protein systems, it sometimes remains necessary to use one of a range of implicit solvent models, such as those based on Generalized Born approaches.[19−22]

In simulations involving explicit water, it is crucial that a balance exists between water−protein and water−water interactions in order to describe correctly the water−protein interface. This balance is ensured by careful parametrization. In the following we consider the parametrization of the CHARMM force field, although other force fields have used similar approaches.

Water and the CHARMM Force Field. In both the CHARMM19[23,24] and CHARMM22[25] force fields, the basis was chosen to be a modified version of the TIP3P water model,[13] since this model provides a satisfactory description of first-shell hydration and the energetics of liquid water while remaining computationally inexpensive. The modification of the original model involved the addition of van der Waals interaction sites to the H atoms,[23,24] but the effects of these additional sites on the properties of the modified water model relative to the original TIP3P model have been found to be small.[26] To differentiate between the original TIP3P model and the CHARMM-modified TIP3P model, we use the acronym mTIP3P to indicate the latter.

The second stage of the parametrization was to determine peptide backbone parameters using the model compound N-methyl acetamide (NMA). The nonbonding parameters for the atoms in NMA (partial charges and van der Waals parameters) were chosen in order to reproduce the binding energy and minimum energy structure of NMA−water and NMA−NMA dimers as determined from ab initio calculations at the HF/6-31G* level. mTIP3P water and NMA can therefore be considered as the foundations on which the rest of the CHARMM force field is built.

Tests of the parametrization included calculation of the molecular volume and heat of solvation of NMA, which were found to be in good agreement with experiment.[25] This agreement was taken to indicate that the solute−solute and solute−solvent interactions are appropriately balanced in the CHARMM22 parameter set.

Recognizing that the solvation energetics are of critical importance for many biomolecular processes, such as protein folding and biomolecular association, it is also interesting to note that the latest parameter sets for the GROMOS force field[27] have been parametrized explicitly to reproduce the experimental solvation free enthalpies of a range of small polar molecules in cyclohexane and in water. More recently, the transferability of these parameters to the calculation of solvation properties in other solvents has been demonstrated.[28]

Recently, there has been a growing interest in comparing force fields and determining which combination(s) of biomolecular force field and water model gives the most satisfactory results.[29−33] These studies have mainly employed thermodynamic criteria in their assessment, such as solvation free energies. Although it is indeed necessary that thermodynamic properties are correctly reproduced, so far little work has been done on examining the details of the water−solute interactions at the atomic level.

Limitations of the Current Force Field. TIP3P (original or modified) is not a perfect water model. In particular, TIP3P water is found to display too little structuring, with the second peak in the oxygen−oxygen radial distribution function (g_{OO}) almost completely absent.[13] The isothermal compressibility is too low, and the coefficient of thermal expansion is too high. It must also be remembered that the model was parametrized for 1 atm and 25 °C. Away from these conditions it must be used with caution. This point is reinforced by noting that the freezing temperature of the TIP3P model has recently been calculated to be 146 K.[34]

The TIP3P model was originally designed for bulk water simulations. Because of this, many-body interactions and

polarization effects are described in an empirical way by increasing the dipole moment of each water molecule relative to the gas phase; the dipole moment of a TIP3P water is 2.35 D, compared to 1.85 D determined experimentally for the gas phase.[35] Because of this, TIP3P is unable to describe correctly the water dimer minimum energy structure; the binding energy is too high; and the O···O distance too short. This suggests that the TIP3P model is not ideal for investigating the details of protein−water interactions, for example, in the case of buried water molecules or water molecules at the protein surface, since it can be expected that polarization effects will be significant in such situations.

It is therefore of significant interest to investigate the behavior of the CHARMM22 force field with water models other than the modified TIP3P model. Once this behavior is understood, it will be possible to choose the most appropriate water model for any given simulation being carried out. For example, this might be the TIP4P/Ew model when Ewald summation is being used,[36] the TIP5P model if the simulations are being carried out close to the water density maximum at 4 °C,[14] TIP4P/Ice if simulations are to be carried out with ice−water coexistence,[37] the Gaussian charge polarizable model (GCPM) for systems under high pressure,[38] or the ab initio, anisotropically polarizable ASP-W2K model if an accurate description of a small number of surface or buried water molecules are of interest.[8]

In the rest of this paper we fix ourselves a more modest aim—to investigate the effect of using the TIP4P and TIP5P models to describe solvent water in biomolecular simulations that use the CHARMM22 force field. The use of the CHARMM22 parameter set with water models other than TIP3P may in principle lead to inconsistencies because the water−protein and protein−protein intermolecular parametrization may not be well balanced. Here, we investigate and assess these potential inconsistencies by examining thermodynamic and structural properties of the different models in a range of test cases.

The work is presented as follows. First, the gas-phase interactions of the water models with themselves and with NMA are investigated in order to assess their ability to reproduce ab initio data and to illustrate the importance of a balanced potential. The free energy of solvation for NMA in the different water models is calculated, together with some structural properties of water around NMA. In addition to NMA, we also consider the solvation of a small number of other model compounds which are representative of amino acid side chains: ethane, benzene, acetate, and guanadinium as well as a small protein, crambin. In light of the results obtained, we then draw some conclusions.

Methods

Geometry optimizations and molecular dynamics simulations were performed using the CHARMM program, version c31b2,[2] and ab initio calculations were performed using the CADPAC suite of programs.[39]

The topology and parameters for NMA and the other solute molecules were taken from the CHARMM22 parameter set.[25] Geometry optimizations were performed using the Conjugate Gradient or Adopted-Basis Newton−Raphson (ABNR) algorithms with a tolerance of 1×10^{-5} kcal/mol Å^{-1} unless otherwise stated. Molecular dynamics simulations were performed in the NVE ensemble at 300 K, following heating and sufficient equilibration. A time step of 1 fs was used. The SHAKE algorithm was used to constrain all bonds to hydrogen,[40] and the water models were treated as rigid.

The solvation free energies were determined as described in ref 41, where the solvation free energies (ΔA) of N-methylacetamide and methylamine in CHARMM-modified TIP3P water were calculated. Briefly, the NMA molecule was positioned at the center of a sphere of water molecules with radius 16 Å, taken from a 70 Å cubic box equilibrated at 300 K. Water molecules within 2.8 Å of any NMA atom were deleted. The NMA molecule was then constrained to the center of the sphere with a harmonic force constant of 1 kcal/mol. The system was simulated using the stochastic boundary method[42] with a reaction region of radius 12 Å, in which the system is propagated using Newtonian dynamics, and a buffer region of radius 4 Å around the reaction region in which the motion is simulated using Langevin dynamics. The Langevin friction coefficient for the oxygen atoms in the buffer region was set to 62 ps^{-1}.

For the remaining solute molecules, the setup was performed in the same way. In each case, the atom constrained to the center of the sphere was as follows: acetate—the carbon atom of the CO_2 group, ethane and benzene—one of the carbon atoms, and guanadinium—the central carbon atom.

Other simulation techniques can also be used to calculate solvation free energies. Price and Brooks used a Monte Carlo method to determine solvation free energies of 40 mono- and disubstituted benzenes,[43] whereas Shirts et al. favored molecular dynamics with periodic boundary conditions.[30] The stochastic boundary method was chosen in this work for direct comparison with the results of ref 41. In addition, this protocol provides satisfactory accuracy while reducing the computational effort required.

Following ref 41, solvation free energies were calculated by performing simulations at λ values of 0.02, 0.1, 0.2, 0.3, 0.4, 0.5, 0.6, 0.7, 0.8, 0.9, and 0.98, where λ represents a coupling coefficient between the solvent and solute which can take values between 0 (full coupling) and 1 (no coupling). At each λ, 100 ps of equilibration was followed by production dynamics for either 1900 ps (for $\lambda = 0.02, 0.98$) or 900 ps (for all other λ).

The solvation free energies (ΔA) were then calculated using either the exponential formula (also known as thermodynamic perturbation, TP)[44] with double-wide sampling or thermodynamic integration (TI).[45] Errors were estimated by calculating the energy over 10 ps batches and obtaining the mean and standard deviation, as in ref 41.

For the simulations of crambin, the high resolution (0.54 Å) X-ray crystal structure was taken from the PDB (1ejg)[46] and imported into the CHARMM program. The protein was solvated in a cubic box of TIP*n*P water (with box length 50 Å), previously equilibrated at 300 K. Water molecules within 2.8 Å of a protein heavy atom were deleted, leaving between 3924 and 3936 water molecules. One hundred steps of steepest descent minimization were used to remove bad contacts. The system was then equilibrated at 300 K for 100

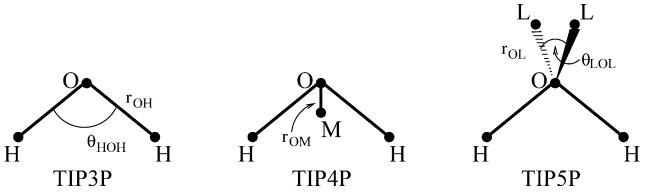

Figure 1. Structural features of the TIP3P, TIP4P, and TIP5P water models.

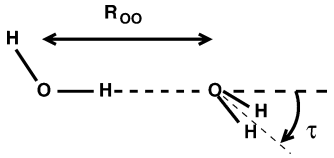

Figure 2. Structure of the linear water dimer.

ps with the protein held fixed, followed by a further 300 ps with no constraints. Two to three ns of dynamics were then calculated. Such simulation lengths are typical of studies involving the comparison of different simulation protocols.[29,47] Simulations were performed in the NVE ensemble with periodic boundary conditions. SHAKE was used to constrain bonds to hydrogen,[40] and the water molecules were treated as rigid. The nonbonded interactions were truncated at 12 Å, with a switch function for the van der Waals interactions and a shift function for the electrostatics.

The truncation of the nonbonded interactions in this work is consistent with the original parametrization procedure used in the development of the TIP water models.[13,14] In comparing and assessing the solvation behavior of different water models, it is necessary to reduce the number of potential sources of error. It is already known that the kinetic and thermodynamic properties of TIP4P water are changed when Ewald summation is included,[36] and this is also likely to occur for TIP3P and TIP5P. However, one cannot assume that such changes will be similar in each case nor even go in the same direction. For these reasons, the nonbonded interactions were truncated as described above.

The TIP*n*P Water Potentials. The TIP*n*P family of water potentials represents a useful test set for investigating the compatibility of alternative water models with the CHARMM22 force field, since they possess many features common to other water potentials, for example, an interaction site at the center of mass or at positions corresponding to lone pairs, but all have the same geometry. They have the general form

$$E_{ab} = \sum_{ij} \frac{q_i q_j e^2}{r_{ij}} + 4\epsilon_O \left[\left(\frac{\sigma_O}{r_{OO}} \right)^{12} - \left(\frac{\sigma_O}{r_{OO}} \right)^{6} \right] \qquad (1)$$

where i and j are the charged sites on molecules a and b separated by a distance r_{ij}, ϵ_O and σ_O are the van der Waals parameters between the two oxygen sites, which are separated by r_{OO}. The O−H bond lengths are fixed at 0.9572 Å and the H−O−H angle is 105.42°, corresponding to the experimental gas-phase values. In the TIP3P model, charges are placed at the O and H atom sites, with a single van der Waals site on O. In the TIP4P model, there is no longer a charge on the O site; instead it is placed at a position corresponding to the molecular center of mass (M), 0.15 Å from the oxygen along the bisector of the H−O−H angle. In the TIP5P model, charges are placed at sites corresponding to lone pair positions (L), 0.7 Å from the oxygen. The three models are shown schematically in Figure 1, and the monomer geometry and parameters are summarized in Table 1.

Table 1. Monomer Geometry and Parameters for the TIP*n*P Potential Functions for use with CHARMM[a]

	TIP3P	mTIP3P	TIP4P	TIP5P
q_H/e	0.417	0.417	0.520	0.241
q_O/e	−0.834	−0.834		
q_M/e			−1.04	
q_L/e				−0.241
σ_{OO}/Å	3.5364	3.5364	3.5399	3.5021
ϵ_O/kcal/mol	0.1521	0.1521	0.1550	0.16
σ_{HH}/Å		0.4490		
ϵ_H/kcal/mol		0.0460		
r_{OH}/Å	0.9572	0.9572	0.9572	0.9572
θ_{HOH}/°	104.52	104.52	104.52	104.52
r_{OM}/Å			0.15	
r_{OL}/Å				0.70
θ_{LOL}/°				109.47

[a] Because of the different definition of the van der Waals interaction energy in CHARMM compared to eq 1, the σ_O parameters differ from those presented in the original papers by a factor of $2^{1/6}$.

Table 2. Geometry and Dimerization Energy for Optimized Linear Water Dimers[a]

donor	acceptor	R_{OO}/Å	τ/°	ΔE/kcal/mol	E_{vdw}
		Homodimers			
TIP3P	TIP3P	2.75	27.3	−6.50	1.74
mTIP3P	mTIP3P	2.77	27.4	−6.55	1.50
TIP4P	TIP4P	2.75	46.2	−6.23	1.80
TIP5P	TIP5P	2.68	51.4	−6.78	2.37
		Heterodimers			
mTIP3P	TIP4P	2.79	50.3	−5.88	1.32
TIP4P	mTIP3P	2.72	21.0	−7.05	2.10
mTIP3P	TIP5P	2.63	51.7	−9.06	3.50
TIP5P	mTIP3P	2.80	30.3	−5.27	1.18
TIP4P	TIP5P	2.53	51.4	−10.60	6.03
TIP5P	TIP4P	2.83	48.8	−4.74	1.00
HF/6-31G*		2.98	56.2	−5.65	
expt[b]		2.98 ± 0.02	57. ± 10	−5.4 ± 0.5	

[a] See Figure 2 for the definition of the structural parameters. In the mixed water dimers, the van der Waals parameters are obtained using the standard combining rules ($\sigma_{AB} = {}^1/_2(\sigma_{AA}/2 + \sigma_{BB}/2)$, $\epsilon_{AB} = \sqrt{(\epsilon_A \epsilon_B)}$). [b] Reference 59 for $(D_2O)_2$.

Results

Water−Water Interactions. In the original papers for the TIP*n*P water models,[13,14] the minimum energy structure of the linear water dimer (constrained to C_s symmetry, with a linear O−H···O hydrogen bond, see Figure 2) was investigated. To demonstrate the importance of a balanced potential, it is instructive to investigate the structure and binding energy of linear water dimers where the donor and acceptor molecules are described with different water models. The results are given in Table 2 and clearly illustrate that such a description is "unbalanced".

It is interesting to note the significant asymmetry in the results when the donor and acceptor molecules in the

Table 3. Interaction Energy Scaling Factors (Ab Initio → Model) for TIP*n*P Water Models

model	scaling factor
mTIP3P	1.16
TIP4P	1.10
TIP5P	1.20

heterodimers are exchanged, in particular with dimers involving a TIP5P molecule. The interaction energies become too large in several cases, coupled to a significantly shortened O···O distance, and vice versa. For the homodimers, the optimized O···O distances are 0.2−0.3 Å shorter than the experimental distance. This difference is due partly to the fact that the TIP*n*P water models were parametrized for bulk water and therefore were not designed to reproduce the water dimer minimum energy geometry.

During the development of the CHARMM22 force field, the water dimer geometry from the mTIP3P model was then compared to the equivalent linear minimum energy conformation obtained from ab initio calculations at the HF/6-31G* level of theory.[48] It was found that the HF/6-31G* interaction energy was smaller than the model interaction energy and the minimum O···O distance longer, effects which were attributed to the small basis set, the low-level of theory used (which neglects correlation contributions), the use of fixed geometries, and the omission of a correction for Basis Set Superposition Error (BSSE). In order to make the energies from ab initio and model calculations directly comparable, the ratio $E_{\text{model}}/E_{\text{ab initio}} = -6.55/-5.65 = 1.16$ was used to scale the ab initio interaction energies.[48] In the same way, it was also assumed that intermolecular distances from model calculations should be 0.2 Å shorter than intermolecular distances obtained from HF/6-31G* calculations (see Table 2).[48] (In this approach, the model calculations were taken as the reference, since the correlation effects, etc. are already included in the water model in an average way.) Had the CHARMM22 force field been parametrized with a different water model, different scaling factors would have been obtained. These are presented in Table 3 and use the data from Table 2. However, as we shall see later, these scale factors are in fact of little use in considering how to use the CHARMM force field with water models other than mTIP3P.

The Interaction of TIP*n*P Water Molecules with NMA. NMA has been widely used as the simplest model of a peptide backbone, and the hydrogen-bonding between water and NMA has been extensively studied.[49−53] Since the first steps of the parametrization of the CHARMM22 force field involved the determination of the geometry and interaction energy of isomers of NMA−water complexes, calculation of equivalent data for alternative water models will give a first indication of whether there are likely to be effects due to an unbalanced potential. However, before considering the NMA−water complexes, it is first useful to consider the conformers of NMA in order to decide which should be used in the solvation calculations.

The Structure of NMA. Considering only the most favorable trans conformation of the peptide bond, and assuming C_s symmetry, a total of four possible conformers are obtained, which can be interconverted through rotation of the methyl groups. These four conformers are illustrated in Figure 3, using the same numbering scheme as in ref 53.

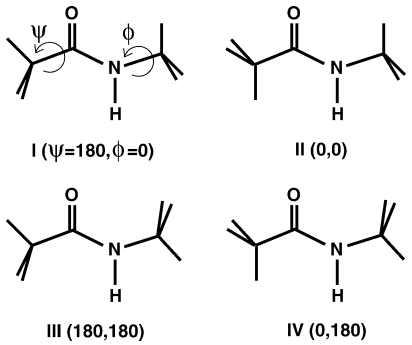

Figure 3. The four conformations of NMA obtained by rotating about the angles ψ and ϕ.

Table 4. Relative Potential Energy as Calculated with CHARMM for Four NMA Conformations, before and after Minimization

conformation	E_{before}/kcal/mol	E_{after}/kcal/mol
I	0.59	0.52
II	0.86	0.79
III	0.0	0.0
IV	0.28	0.26

All four conformers were constructed automatically in the CHARMM program, and their energy was minimized. The relative energies before and after minimization are given in Table 4. It can be seen that CHARMM finds isomer III to be the most stable, followed by IV, I, and II, both before and after minimization. Isomer III corresponds to the structure as reported by gas-phase electron diffraction in 1973.[54] Although this experimental structure was obtained with good precision, several of the assumptions which were necessary to enable interpretation of the experimental data have since been found to be incorrect.[49,53] Ab initio calculations (MP2/6-31G*,[49] B3LYP/6-311++G(2d,2p),[51] B3LYP/6-31+G(d,p)[53]) have consistently shown that isomer III is not the most stable conformation, with isomers II and IV being the isoenergetic minimum energy states for isolated NMA. For hydrated NMA, isomer IV is found to be the minimum energy conformation.[51,53] However, for completeness, we have studied water−NMA complexes involving all four conformations.

Water−NMA Complexes. We have determined the interaction energy and minimum energy geometry for water−NMA complexes in a way as consistent as possible with the method described in the CHARMM22 paper.[25] Three water−NMA isomers are considered here and are depicted in Figure 4 (the original CHARMM paper considered only two conformers, OHO1 and NHO). In each case, the NMA moiety was fixed in the appropriate CHARMM-optimized geometry (the water models are rigid by design), and two intermolecular degrees of freedom were optimized; namely, the H···O hydrogen bond distance, denoted R (where H and O can belong to either water or NMA), and the C−O···O or N···O−(HOH bisector) angle, θ. The hydrogen bond was

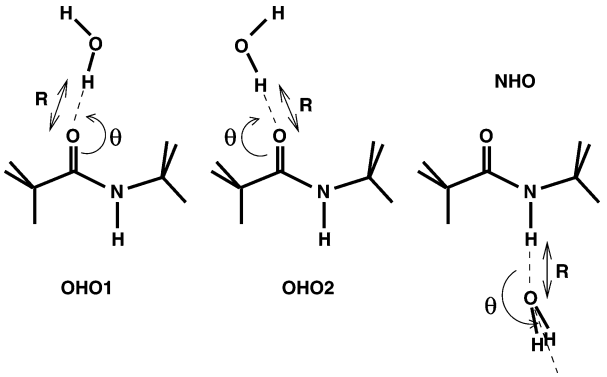

Figure 4. The three NMA−water conformations considered, denoted as OHO1, OHO2, and NHO, with the optimized degrees of freedom R and θ.

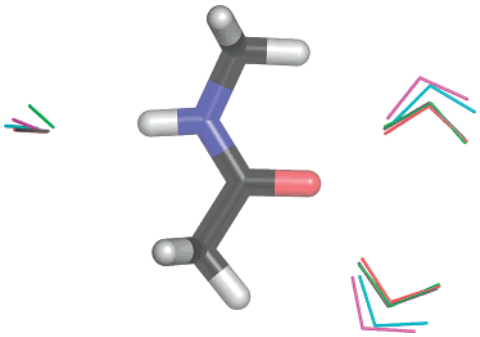

Figure 5. Superposition of NMA···water complexes after optimization of all intermolecular degrees of freedom from model and ab initio calculations. The water molecules are color-coded as follows: mTIP3P − black, TIP4P − red, TIP5P − green, HF/6-31G* − cyan, MP2/6-31G* − magenta. For clarity, the positions of the lone pairs (TIP4P and TIP5P) are not shown. All structures have C_s symmetry.

constrained to be linear, and all calculations were performed with C_s symmetry.

To assess the quality of the structures obtained, the same two degrees of freedom were optimized using ab initio calculations at the HF/6-31G* level (as in the original CHARMM paper) and at the MP2/6-31G* level. The NMA and water geometries were fixed in the optimized geometries given by CHARMM. In Table 5 we present the results for NMA−mTIP3P, together with ab initio data for comparison. As in the original CHARMM parametrization procedure, ab initio interaction energies were not corrected for BSSE.

Upon inspection of Table 5, several features are apparent. First the choice of NMA conformation (I,II,III,IV) does not significantly affect the energy or structural details of the model calculations. The complexes OHO1 and OHO2 are close in energy, with the OHO1 structure slightly more stable than OHO2 for all NMA conformations except conformation III, in which OHO1 and OHO2 are almost isoenergetic. The binding energies of the OHO conformations are found to be between 0.9 and 1.7 kcal/mol larger than the binding energy of the NHO conformation.

There is good agreement between the structural features of the model and HF calculations. The distance R is in general overestimated by around 0.2 Å in the HF calculations, for the reasons described above. The angle θ is reproduced to within 9°. Although the ordering of stability is not always reproduced by the HF calculations, the OHO conformations are still found to be close in energy, while the binding energy of the NHO complex is approximately 2 kcal/mol smaller. In these calculations, the scaled energy (using a factor of 1.16, as described above) is not consistently closer to the model energy than the unscaled energy, except for the NHO complexes. The fact that the scaled energies presented here are not in exact agreement with the scaled energies presented in the original CHARMM22 paper[25] is due to the use of slightly different geometries for the NMA moiety.

In moving from the HF calculations to the MP2 level of theory, the distance R becomes shorter, as expected. The angles in the OHO complexes remain fairly close to those from the HF and model calculations. On the other hand, θ in the NHO complexes moves significantly (up to 35°) away from the approximately linear geometry found in the model and HF calculations. This strongly suggests that the mTIP3P model is indeed not capable of reproducing the details of gas-phase interactions.

Equivalent calculations were carried out for the TIP4P and TIP5P water models, and the results are presented in Table 6. Some interesting observations can be made. For all three water models, the minimized geometries are very similar, with θ varying by a maximum of 9° and R by a maximum of 0.07 Å as the water model is changed. When mTIP3P is changed to TIP4P, the binding energies of the OHO complexes increase by 0.2−0.3 kcal/mol, while the binding energies of the NHO complexes are reduced by around 0.6 kcal/mol. However, the binding energies with the TIP5P model behave quite differently. The OHO complexes have a binding energy between 6 and 7 kcal/mol, significantly smaller than found for mTIP3P and TIP4P. On the other hand, the NHO complexes are more strongly bound than with mTIP3P and TIP4P and are even more strongly bound than some of the OHO complexes. This is in disagreement with the trends found in the ab initio calculations (both HF and MP2). Since there is no systematic difference between the water models, this also indicates that the use of a scale factor calculated for a given water model in order to bring ab initio binding energies into agreement with energies from model force field calculations cannot be generalized to other water models.

The energy minimizations with two degrees of freedom presented above are useful for direct comparisons between models, but it is possible that these structures differ significantly from those found when all the intermolecular degrees of freedom are optimized. For this reason, all intermolecular degrees of freedom were optimized (in principle there are six intermolecular degrees of freedom, but the presence of a symmetry plane in all cases reduces this number to three) while keeping the monomers in their CHARMM-optimized geometry. For comparison, we also performed equivalent ab initio calculations at the HF/6-31G* and MP2/6-31G* levels.

The binding energies obtained for NMA conformation I (the others NMA conformations lead to very similar results) are given in Table 7, and the optimized structures are superimposed in Figure 5.

Table 5. Interaction Energies and Structural Data for NMA−mTIP3P Complexes[a]

conformation		model			HF				MP2		
		R/Å	*θ*/°	*E*	*R*/Å	*θ*/°	*E*	E_{scaled}	*R*/Å	*θ*/°	*E*
I	OHO1	1.76	145	−7.70	1.97	143	−7.03	−8.15	1.91	139	−8.73
	OHO2	1.76	126	−7.26	1.97	122	−7.25	−8.41	1.92	117	−8.78
	NHO	1.92	174	−6.18	2.12	167	−5.14	−5.96	2.06	167	−6.82
II	OHO1	1.76	145	−7.71	1.96	144	−7.10	−8.23	1.91	139	−8.79
	OHO2	1.77	122	−7.26	1.97	117	−7.53	−8.73	1.93	110	−9.14
	NHO	1.93	172	−6.30	2.14	179	−5.48	−6.36	2.03	215	−7.55
III	OHO1	1.76	137	−8.07	1.98	135	−7.45	−8.64	1.94	131	−9.29
	OHO2	1.76	126	−7.27	1.97	122	−7.23	−8.39	1.92	117	−8.75
	NHO	1.92	174	−6.18	2.12	173	−5.26	−6.10	2.01	167	−6.94
IV	OHO1	1.76	137	−8.08	1.98	135	−7.53	−8.73	1.94	131	−9.36
	OHO2	1.76	122	−7.26	1.98	117	−7.49	−8.69	1.94	110	−9.09
	NHO	1.92	172	−6.32	2.13	183	−5.61	−6.50	2.02	215	−7.66

[a] Energies are given in kcal/mol. Ab initio calculations used the 6-31G* basis set.

Table 6. Interaction Energies and Structural Data for NMA−TIP*n*P Complexes[a]

conformation		mTIP3P			TIP4P			TIP5P		
		R/Å	*θ*/°	*E*	*R*/Å	*θ*/°	*E*	*R*/Å	*θ*/°	*E*
I	OHO1	1.76	145	−7.70	1.72	147	−7.94	1.79	145	−6.42
	OHO2	1.76	126	−7.26	1.73	129	−7.43	1.79	126	−6.05
	NHO	1.92	174	−6.18	1.95	171	−5.53	1.86	150	−6.67
II	OHO1	1.76	145	−7.71	1.72	147	−7.95	1.78	146	−6.42
	OHO2	1.77	122	−7.26	1.73	126	−7.42	1.80	121	−6.07
	NHO	1.93	172	−6.30	1.96	169	−5.66	1.87	150	−6.86
III	OHO1	1.76	137	−8.07	1.72	139	−8.28	1.79	137	−6.78
	OHO2	1.76	126	−7.27	1.73	129	−7.44	1.79	126	−6.06
	NHO	1.92	174	−6.18	1.95	171	−5.53	1.86	150	−6.67
IV	OHO1	1.76	137	−8.08	1.72	139	−8.29	1.79	137	−6.78
	OHO2	1.76	122	−7.26	1.73	127	−7.43	1.80	121	−6.07
	NHO	1.92	172	−6.32	1.96	170	−5.67	1.87	150	−6.87

[a] Some of the data from Table 5 are reproduced again here to aid in comparison. Energies are given in kcal/mol.

Table 7. Binding Energies in kcal/mol for NMA···Water Complexes Following Optimization of All Intermolecular Degrees of Freedom for NMA Conformation I[a]

conformation	mTIP3P	TIP4P	TIP5P	HF	MP2
OHO1	−7.75	−7.94	−6.51	−7.12	−8.95
OHO2	−7.27	−7.44	−6.09	−7.41	−9.10
NHO	−6.18	−5.53	−6.92	−5.14	−6.82

[a] Ab initio calculations used the 6-31G* basis set.

Table 8. Free Energies of Solvation (ΔA_{solv}) of NMA in Various Water Models in kcal/mol

water model	TP	TI	mean
mTIP3P	−11.81 ± 0.05	−11.60 ± 0.04	−11.71 ± 0.03
TIP4P	−10.22 ± 0.07	−9.94 ± 0.06	−10.08 ± 0.05
TIP5P	−10.54 ± 0.06	−10.27 ± 0.06	−10.41 ± 0.04
mTIP3P[a]	−10.4 ± 0.09	−11.3 ± 0.05	−10.85 ± 0.07
expt[b]			−10.1

[a] Reference 41. [b] Reference 60.

Although the binding energies for the TIP*n*P models vary, it can be seen that the optimized structures are in fact very similar to each other. The exception is the N−H···O complex with the TIP5P model, for which the presence of lone-pair sites at the tetrahedral positions makes the H−O−H plane bend away from the N−H···O vector. Nevertheless, it is interesting to note that this bending is also apparent in the MP2/6-31G* structure (but not in the HF/6-31G* structure) although the N−H···O distance is underestimated for the TIP5P model, for the reasons discussed above. For the O−H···O complexes, all models are approximately equally distant from the ab initio structures.

Solvation Free Energy of NMA in TIP*n*P Water. To assess the effect of the choice of water model on thermodynamic properties, the solvation free energy of NMA in mTIP3P, TIP4P, and TIP5P was calculated using both the thermodynamic perturbation and thermodynamic integration methods as described in the 'Methods' section. The resulting solvation free energies are given in Table 8.

In each case, the value obtained from TP is 0.2−0.3 kcal/mol larger in magnitude than the value from TI, and this difference gives an indication of the accuracy of the calculations. The average ΔA_{solv} for TIP4P and TIP5P are similar and lie within 0.3 kcal/mol of the experimental determination. The value for mTIP3P is 1.3 kcal/mol larger in magnitude than the TIP5P value and around 1.6 kcal/mol larger than found in experiment. The values obtained in this work for mTIP3P are slightly larger than those obtained in ref 41 but lie within 0.5 kcal/mol of the value previously

Table 9. Free Energies of Solvation (ΔA_{solv}) for Neutral Solutes in Various Water Models in kcal/mol[a]

solute	mTIP3P	TIP4P	TIP5P	expt
ethane	-0.04 ± 0.03	$+0.93 \pm 0.03$	-0.09 ± 0.03	1.833[b]
benzene	-5.09 ± 0.04	-3.35 ± 0.05	-4.37 ± 0.04	-0.767[c]

[a] The figures given are the mean of the values calculated with TP and TI, for which the individual values show similar trends to those observed for NMA. [b] ΔG_{solv} from ref 61. [c] ΔG_{solv} from ref 62.

obtained using TI.[41] The difference in the values obtained with TI and TP in this study is of the order of 0.2 kcal/mol, compared to 0.9 kcal/mol in ref 41.

The solvation free energies obtained for TIP4P and TIP5P are closer to the experimental value than the value for mTIP3P. Once again, this suggests that the combination of the CHARMM force field with the TIP4P and TIP5P water models has the potential to give reasonable results.

We also calculated the free energies of solvation for two neutral and nonpolar solutes; ethane and benzene, which are related to the side chains of isoleucine and phenylalanine. The results are presented in Table 9. The calculated solvation free energies show only small variation with water model, as would be expected for neutral, nonpolar solutes. In both cases, the TIP4P model gives values closest to the experimentally determined value for ΔG_{solv}; however, the values are not particularly satisfactory. The differences are partly due to comparing calculated ΔA values with experimental ΔG values but also indicate that solvation energies for small molecules are not reproduced particularly well[30,32] unless the force field has been designed to reproduce solvation thermodynamics.[27,28]

Given the well-known difficulties in calculating solvation free energies for charged molecules,[55,56] we do not attempt to calculate any values for analogues of charged amino acids here.

Further insight can be obtained from the extensive study of solvation free energies in ref 32. In this study, the OPLS-AA force field[5] was used to investigate the solvation free energies of (neutral) amino acid analogs in different water models. Although NMA was not explicitly studied, acetamide was chosen as the analog of asparagine. For the five water models investigated (TIP3P, SPC, TIP4P, SPC/E, and TIP4P-Ew), the solvation free energy of acetamide was found to vary over a range of 0.2 kcal/mol (between -8.32 (SPC/E) and -8.53 (SPC) kcal/mol). The values for TIP3P and TIP4P were identical to within the uncertainty of the simulations (-8.51 and -8.52 kcal/mol, respectively). This agreement may be due to the fact that the OPLS potential was originally designed to be compatible with the TIP3P, TIP4P, and SPC water models.[57] Although the parameters for acetamide differ between the OPLS-AA and CHARMM22 force fields, this nevertheless suggests that, for a given force field, the difference in solvation energy with different water models (at least among the models considered) is small. For the worst cases in the study of ref 32, *p*-cresol and 3-methylindole (analogs of tyrosine and tryptophan, respectively), the spread of predicted solvation free energies was found to be 0.66 and 0.86 kcal/mol. In most cases among the analogs, TIP3P (the original TIP3P model, not the CHARMM-modified TIP3P model) was found to give the lowest limit in 10 out of 15 cases, suggesting that TIP3P often gives a lower (i.e., smaller if positive, more negative if negative) estimate of the solvation free energy, in agreement with the results from this work. The highest values were not dominated by one particular water model.

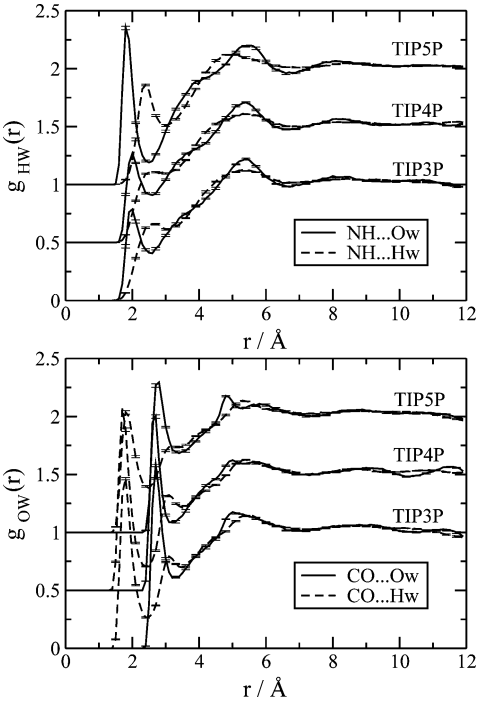

Figure 6. Solvent distribution functions $g_{OW}(r)$ and $g_{HW}(r)$, where H and O are NMA atoms and *W* is a water atom (H or O) for NMA in TIP*n*P water at 300 K. The functions for TIP4P and TIP5P have been displaced vertically for clarity. The error bars show the error on the mean determined by dividing the trajectory into ten equal sections and calculating the solvent distribution function for each section.

Structural Properties of TIP*n*P Solvation. In addition to considering the interaction of individual water molecules with NMA and the calculation of thermodynamic properties, it is also instructive to investigate the structure of the water around the NMA and, in particular, the solvent distribution functions around the N−H hydrogen bond donor and the C−O hydrogen bond acceptor moieties. The NH−W and CO−W distribution functions (where W is a water atom, either oxygen or hydrogen) were calculated from a 1.9 ns trajectory using stochastic boundary conditions (as described in the 'Methods' section) for each of the TIP water models. The results are shown in Figure 6.

The CO−W distribution functions are almost identical for the three models. This is because the H atom parameters are similar in all three cases. For the NH−W distribution functions, the mTIP3P and TIP4P profiles are similar, whereas the TIP5P profile is significantly different, due to the presence of lone pairs in the TIP5P model which become involved in the NH−O interaction. The NH−O peak in the TIP5P distribution function is sharper and larger than for mTIP3P and TIP4P, indicating a larger number of water molecules involved in hydrogen bonds at this site. The O atoms in the first hydration shell are also slightly closer to the NH donor, with a peak position of 1.9 Å for TIP5P

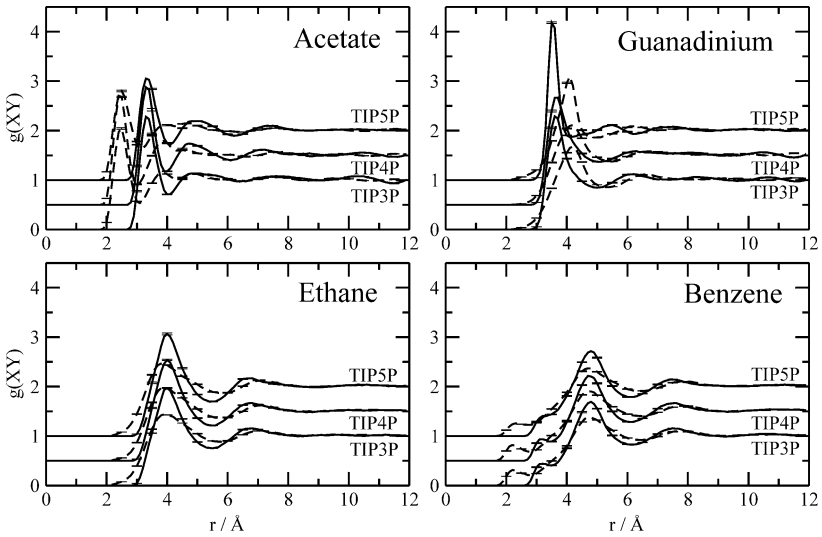

Figure 7. Solvent distribution functions $g_{XY}(r)$ for acetate, guanadinium, ethane, and benzene in TIP*n*P water at 300 K, where Y is a water atom (O − solid line, H − dashed line) and X is a reference atom or site (see text for details). The functions for TIP4P and TIP5P have been displaced vertically for clarity. The error bars show the error on the mean determined by dividing the trajectory into ten equal sections and calculating the solvent distribution function for each section.

compared to 2.1 Å for TIP4P and 2.0 Å for mTIP3P. Which of these descriptions is closer to reality is not yet known. A recent experimental neutron diffraction study has provided detailed structural information for solvated L-glutamic acid;[58] a similar study of NMA would provide the experimental data necessary to evaluate these distribution functions. Beyond the first solvation shell, the structure of the distribution functions are similar, although there is little useful information beyond the first peak and trough. The feature at around $r = 4.8$ Å in the CO−O distribution functions can be assigned to the first solvation shell of the NH group on the other side of the molecule.

In ref 32, no analogs of charged amino acids were considered. Such cases are likely to provide a tough challenge for the water models, since hydrogen-bonding between the solute and solvent will be stronger in these cases than for neutral species. To investigate this aspect, we calculated solvent distribution functions around two charged model compounds, acetate and guanadinium, which are closely related to the side chains of the amino acids aspartate and arginine. We also considered two neutral and nonpolar solutes, ethane and benzene, which are similar in nature to the side chains of isoleucine and phenylalanine.

The distribution functions for acetate (around the carbon atom of the CO_2 group), guanadinium, benzene, and ethane (around the geometric center of the molecule) are shown in Figure 7. For the neutral, nonpolar solutes, the profiles for all water models are almost identical. However for charged solutes, the TIP5P model behaves differently; for guanadinium, g(XO) displays a very large first peak, corresponding to strong NH−O interactions. The opposite can be seen for acetate, where the solute−water hydrogen bonds are weaker for TIP5P than for the other models.

Dynamics of Crambin in TIP*n*P Water. One potential side effect of using an inappropriate water model could be instabilities in the protein structure or even unfolding. For this reason, simulations of the small protein crambin were performed using the TIP*n*P water models. To our knowledge, these are the first simulations of a biomolecular system performed using the TIP5P water model.

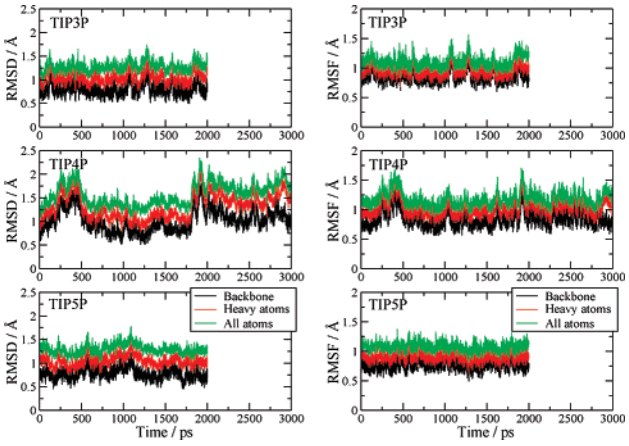

Figure 8. Left: Root-mean-square deviation (rmsd) of the protein structure from the crystal structure during the simulations. Right: Root-mean-square fluctuation (rmsf) of the protein about the mean structure over the simulations.

In Figure 8(left), the root-mean-square deviation (rmsd) is presented as a function of time from each of the simulations. The rmsd is taken with respect to the crystal structure.[46] The protein remains stable in the mTIP3P and TIP5P simulations, with average backbone rmsd values of 0.80 and 0.78 Å, respectively. The average backbone rmsd from the TIP4P simulation is slightly larger, with a value of 0.96 Å, due to the fluctuations observed at $t = 250-500$ ps and $t = 1750-2000$ ps. To check that this was not due to unfolding of the protein, the trajectory was continued for a further nanosecond, during which the rmsd was found to remain stable, with a mean value of 1.01 Å.

The root-mean-square fluctuation of the protein along the trajectories (determined with respect to the corresponding mean structure) is shown in Figure 8 (right) and also indicates that the structure is stable in all three simulations. Decomposition of the rmsf into contributions per residue reveals

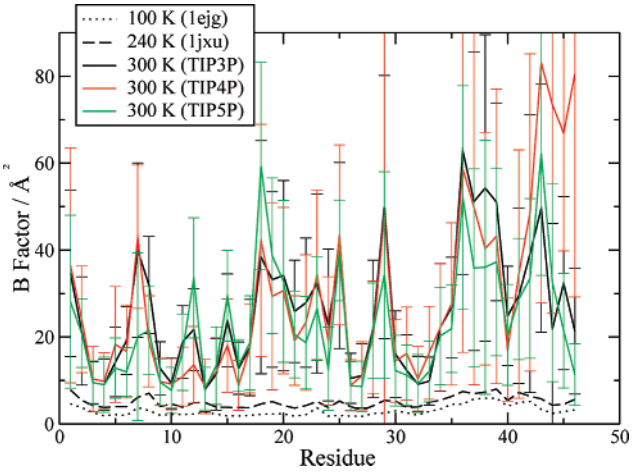

Figure 9. Residue fluctuations (plotted as thermal *B*-factors) from the simulations and from two crystal structures. The error bars represent ±1 standard deviation about the mean.

that the fluctuations in the rmsd from the TIP4P trajectory are due to motion of sections of the β-sheet, between residues 42 and 46, as shown in Figure 9. Comparison with thermal *B*-factors from crystal diffraction data reveal common features (the same flexible and rigid regions) but are not in quantitative agreement. This is because the simulations were performed at 300 K, whereas the crystallographic data was measured at 100 K (1ejg) and 240 K (1jxu).

Discussion and Conclusions

In this paper we have investigated various features of the interaction between N-methylacetamide, other small solute molecules, and a small protein (all represented with the CHARMM22 force field), with three different water models, mTIP3P, TIP4P, and TIP5P, in order to assess whether the use of the CHARMM22 force field with water models not considered in the original parametrization leads to an imbalance in simulations.

Results obtained for NMA−water complexes with mTIP3P and TIP4P show very similar structural and energetic properties. In addition, the free energy of solvation for NMA in TIP4P appears to be closer to the experimental value than that calculated with mTIP3P. This is not surprising, since TIP4P provides a better description of the bulk water structure, while not significantly distorting the details of the NMA−water interactions. It therefore seems likely that TIP4P will give reasonable local structural and energetic results when used as a solvent model together with the CHARMM22 protein force field.

TIP5P, on the other hand, behaves differently to mTIP3P and TIP4P, mainly due to the presence of lone pair sites on the oxygen atom. These alter the details of the interactions, in particular when the water oxygen acts as a hydrogen acceptor. This can be seen most clearly in the NH···O distribution function for NMA and guanadinium. Whether this is due to the functional form of the TIP5P model itself (i.e., the presence of lone pair sites) or to the TIP5P parameters remains to be investigated.

Despite the differences observed for TIP5P in the details of the solvation structure, simulations of crambin show that the protein remains stable in TIP5P water as well as in mTIP3P and TIP4P water. This gives a first indication that TIP5P may be used (with care) in biomolecular simulations using the CHARMM22 force field. This is significant, since TIP5P will provide a much better description than TIP3P in simulations at low temperature. Even at room temperature, the use of TIP5P can be expected to give a significant improvement over TIP3P, since the thermodynamic and kinetic properties of the TIP5P model are much closer to those of real water than those of TIP3P. The additional computational expense required for the five-point model is largely offset by the computing power now available.

Further comparison of simulation results with experimental data will be required in order to assess which of the water models gives the best description of the details of the protein−water interface. Furthermore, extensive work will be necessary examining a wide range of structural, dynamical, and thermodynamical properties of small and large biomolecules in solution before a clear picture emerges of the relative behavior of different standard water molecular mechanics models with any given macromolecular force field. However, the present results, although limited in the force fields tested and properties examined, do suggest that such research will be potentially fruitful.

Acknowledgment. D.R.N. is grateful to the Swiss National Science Foundation (SNF) for the award of an Advanced Research Fellowship.

References

(1) Teeter, M. M. *Annu. Rev. Biophys. Biophys. Chem.* **1991**, *20*, 577−600.

(2) Brooks, B. R.; Bruccoleri, R. E.; Olafson, B. D.; States, D. J.; Swaminathan, S.; Karplus, M. *J. Comput. Chem.* **1983**, *4*, 187−217.

(3) Weiner, S. J.; Kollman, P. A.; Case, D. A.; Singh, U. C.; Ghio, C.; Alagona, G.; Profeta, S.; Weiner, P. *J. Am. Chem. Soc.* **1984**, *106*, 765−784.

(4) Hermans, J.; Berendsen, H. J. C.; van Gunsteren, W. F.; Postma, J. P. M. *Biopolymers* **1984**, *23*, 1513−1518.

(5) Jorgensen, W. L.; Maxwell, D. S.; Tirado-Rives, J. *J. Am. Chem. Soc.* **1996**, *118*, 11225−11236.

(6) Millot, C.; Stone, A. J. *Mol. Phys.* **1992**, *77*, 439−462.

(7) Millot, C.; Soetens, J.-C.; Martins Costa, M. T. C.; Hodges, M. P.; Stone, A. J. *J. Phys. Chem. A* **1998**, *102*, 754−770.

(8) Nutt, D. R.; Stone, A. J. *J. Chem. Phys.* **2002**, *117*, 800−807.

(9) Hodges, M. P.; Stone, A. J.; Xantheas, S. S. *J. Phys. Chem. A* **1997**, *101*, 9163−9168.

(10) Engkvist, O.; Stone, A. J. *J. Chem. Phys.* **1999**, *110*, 12089−12096.

(11) Sadtchenko, V.; Ewing, G. E.; Nutt, D. R.; Stone, A. J. *Langmuir* **2002**, *18*, 4632−4636.

(12) Nutt, D. R.; Stone, A. J. *Langmuir* **2004**, *20*, 8715−8720.

(13) Jorgensen, W. L.; Chandrasekhar, J.; Madura, J. D.; Impey, R. W.; Klein, M. L. *J. Chem. Phys.* **1983**, *79*, 926−935.

(14) Mahoney, M. W.; Jorgensen, W. L. *J. Chem. Phys.* **2000**, *112*, 8910−8922.

(15) Berendsen, H. J. C.; Postma, J. P. M.; von Gunsteren, W. F.; Hermans, J. Interaction models for water in relation to protein hydration. In *Intermolecular Forces*; Pullman, B., Ed.; D. Reidel: Dordrecht, Holland, 1981.

(16) Berendsen, H. J. C.; Grigera, J. R.; Straatsma, T. P. *J. Phys. Chem.* **1987**, *91*, 6269−6271.

(17) Stillinger, F. H.; Rahman, A. *J. Chem. Phys.* **1974**, *60*, 1545.

(18) Guillot, B. *J. Mol. Liq.* **2002**, *101*, 219−260.

(19) Still, W. C.; Tempczyk, A.; Hawley, R. C.; Hendrickson, T. *J. Am. Chem. Soc.* **1990**, *112*, 6127−6129.

(20) Schaefer, M.; Karplus, M. *J. Phys. Chem.* **1996**, *100*, 1578−1599.

(21) Lee, M. S.; Feig, M.; Salsbury, F. R.; Brooks, C. L. *J. Comput. Chem.* **2003**, *24*, 1348−1356.

(22) Koppole, S.; Smith, J. C.; Fischer, S. *J. Mol. Biol.* **2006**, *361*, 604−616.

(23) Reiher, W. E. Thesis, Harvard University, 1985.

(24) Neria, E.; Fischer, S.; Karplus, M. *J. Chem. Phys.* **1996**, *105*, 1902−1921.

(25) MacKerell, A. D., Jr. et al. *J. Phys. Chem. B* **1998**, *102*, 3586−3616.

(26) Mark, P.; Nilsson, L. *J. Phys. Chem. A* **2001**, *105*, 9954−9960.

(27) Oostenbrink, C.; Villa, A.; Mark, A. E.; van Gunsteren, W. F. *J. Comput. Chem.* **2004**, *25*, 1656−1676.

(28) Geerke, D. P.; van Gunsteren, W. F. *Phys. Chem. Chem. Phys.* **2006**, *7*, 671−678.

(29) Price, D. J.; Brooks, C. L., III *J. Comput. Chem.* **2002**, *23*, 1045−1057.

(30) Shirts, M. R.; Pitera, J. W.; Swope, W. C.; Pande, V. S. *J. Chem. Phys.* **2003**, *119*, 5740−5761.

(31) Kim, B.; Young, T.; Harder, E.; Friesner, R. A.; Berne, B. J. *J. Phys. Chem. B* **2005**, *109*, 16529−16538.

(32) Shirts, M. R.; Pande, V. S. *J. Chem. Phys.* **2005**, *2005*, 134508.

(33) Hess, B.; van der Vegt, N. F. A. *J. Phys. Chem. B* **2006**, *110*, 17616−17626.

(34) Vega, C.; Sanz, E.; Abascal, J. L. F. *J. Chem. Phys.* **2005**, *122*, 114507.

(35) Clough, S. A.; Beers, Y.; Klein, G. P.; Rothman, L. S. *J. Chem. Phys.* **1973**, *59*, 2254−2259.

(36) Horn, H. W.; Swope, W. C.; Pitera, J. W.; Madura, J. D.; Dick, T. J.; Hura, G. L.; Head-Gordon, T. *J. Chem. Phys.* **2004**, *120*, 9665−9678.

(37) Abascal, J. L. F.; Sanz, E.; García Fernández, R.; Vega, C. *J. Chem. Phys.* **2005**, *122*, 234511.

(38) Paricaud, P.; Předota, M.; Chialvo, A. A.; Cummings, P. T. *J. Chem. Phys.* **2005**, *122*, 244511.

(39) Amos, R. D. *CADPAC: The Cambridge Analytic Derivatives Package, Issue 6*; Technical Report; University of Cambridge: 1995. A suite of quantum chemistry programs developed by R. D. Amos with contributions from I. L. Alberts, J. S. Andrews, S. M. Colwell, N. C. Handy, D. Jayatilaka, P. J. Knowles, R. Kobayashi, K. E. Laidig, G. Laming, A. M. Lee, P. E. Maslen, C. W. Murray, J. E. Rice, E. D. Simandiras, A. J. Stone, M. D. Su, and D. J. Tozer.

(40) Ryckaert, J. P.; Ciccotti, G.; Berendsen, H. J. C. *J. Comp. Phys.* **1977**, *23*, 327−341.

(41) Wan, S.; Stote, R. H.; Karplus, M. *J. Chem. Phys.* **2004**, *121*, 9539−9548.

(42) Brooks, C. L., III; Karplus, M. *J. Chem. Phys.* **1983**, *79*, 6312−6325.

(43) Price, D. J.; Brooks, C. L., III. *J. Comput. Chem.* **2005**, *26*, 1529−1541.

(44) Zwanzig, R. W. *J. Chem. Phys.* **1954**, *22*, 1420−1426.

(45) Straatsma, T. P.; Berendsen, H. J. C. *J. Chem. Phys.* **1988**, *89*, 5876−5886.

(46) Jelsch, C.; Teeter, M. M.; Lamzin, V.; Pichon-Pesme, V.; H. B. R. Lecomte, C. *Proc. Natl. Acad. Sci.* **2000**, *97*, 3171−3176.

(47) van der Spoel, D.; van Maaren, P. J. *J. Chem. Theory Comput.* **2006**, *2*, 1−11.

(48) MacKerrell, A. D. Jr.; Karplus, M. *J. Phys. Chem.* **1991**, *95*, 10559−10560.

(49) Guo, H.; Karplus, M. *J. Phys. Chem.* **1992**, *96*, 7273−7287.

(50) Baudry, J.; Smith, J. C. *J. Mol. Struct. (Theochem*) **1994**, *308*, 103−113.

(51) Han, W.-G.; Suhai, S. *J. Phys. Chem.* **1996**, *100*, 3942−3949.

(52) Buck, M.; Karplus, M. *J. Phys. Chem. B* **2001**, *105*, 11000−11015.

(53) Mennucci, B.; Martínez, J. M. *J. Phys. Chem. B* **2005**, *109*, 9818−9829.

(54) Kitano, M.; Fukuyama, T.; Kuchitsu, K. *Bull. Chem. Soc. Jpn.* **1973**, *46*, 384−387.

(55) Kelly, C. P.; Cramer, C. J.; Truhlar, D. G. *J. Phys. Chem. B* **2006**, *110*, 16066−16081.

(56) Kastenholz, M. A.; Hünenberger, P. H. *J. Chem. Phys.* **2006**, *124*, 224501.

(57) Jorgensen, W. L.; Tirado-Rives, J. *J. Am. Chem. Soc.* **1988**, *110*, 1657−1666.

(58) McLain, S. E.; Soper, A. K.; Watts, A. *J. Phys. Chem. B* **2006**, *110*, 21251−21258.

(59) Fellers, R. S.; Leforestier, C.; Braly, L. B.; Brown, M. G.; Saykally, R. J. *Science* **1999**, *284*, 945−948.

(60) Wolfenden, R. *Biochemistry* **1978**, *17*, 201−204.

(61) Wilhelm, E.; Battino, R.; Wilcock, R. J. *Chem. Rev.* **1977**, *77*, 219−262.

(62) Wauchope, R. D.; Haque, R. *Can. J. Chem.* **1972**, *50*, 133.

CT700053U